

# Regulation of Gene Expression during the Onset of Ligninolytic Oxidation by *Phanerochaete chrysosporium* on Spruce Wood

Premsagar Korripally,<sup>a</sup> Christopher G. Hunt,<sup>b</sup> Carl J. Houtman,<sup>b</sup> Don C. Jones,<sup>b</sup> Peter J. Kitin,<sup>b</sup> Dan Cullen,<sup>b,c</sup> Kenneth E. Hammel<sup>b,c</sup>

Department of Biotechnology, Mahatma Gandhi University, Nalgonda, India<sup>a</sup>; U.S. Forest Products Laboratory, Madison, Wisconsin, USA<sup>b</sup>; Department of Bacteriology, University of Wisconsin, Madison, Wisconsin, USA<sup>c</sup>

Since uncertainty remains about how white rot fungi oxidize and degrade lignin in wood, it would be useful to monitor changes in fungal gene expression during the onset of ligninolysis on a natural substrate. We grew *Phanerochaete chrysosporium* on solid spruce wood and included oxidant-sensing beads bearing the fluorometric dye BODIPY 581/591 in the cultures. Confocal fluorescence microscopy of the beads showed that extracellular oxidation commenced 2 to 3 days after inoculation, coincident with cessation of fungal growth. Whole transcriptome shotgun sequencing (RNA-seq) analyses based on the v.2.2 *P. chrysosporium* genome identified 356 genes whose transcripts accumulated to relatively high levels at 96 h and were at least four times the levels found at 40 h. Transcripts encoding some lignin peroxidases, manganese peroxidases, and auxiliary enzymes thought to support their activity showed marked apparent upregulation. The data were also consistent with the production of ligninolytic extracellular reactive oxygen species by the action of manganese peroxidase-catalyzed lipid peroxidation, cellobiose dehydrogenase-catalyzed Fe<sup>3+</sup> reduction, and oxidase-catalyzed H<sub>2</sub>O<sub>2</sub> production, but the data do not support a role for iron-chelating glycopeptides. In addition, transcripts encoding a variety of proteins with possible roles in lignin fragment uptake and processing, including 27 likely transporters and 18 cytochrome P450s, became more abundant after the onset of extracellular oxidation. Genes encoding cellulases showed little apparent upregulation and thus may be expressed constitutively. Transcripts corresponding to 165 genes of unknown function accumulated more than 4-fold after oxidation commenced, and some of them may merit investigation as possible contributors to ligninolysis.

The biodegradation of lignocellulose requires the disruption of its lignin, which shields the metabolically assimilable polysaccharides in this recalcitrant natural composite. Although a variety of microorganisms can attack lignocellulose, white rot basidiomycetes are uniquely efficient at this process, cleaving the recalcitrant intermonomer linkages of lignin via extracellular oxidative mechanisms and mineralizing many of the resulting fragments to carbon dioxide (1). Considerable progress has been made in understanding this process in the extensively researched white rot fungus *Phanerochaete chrysosporium*, which expresses important components of its ligninolytic system in response to nutrient limitation as part of its secondary metabolism. Biochemical and genetic evidence points to an important role in *P. chrysosporium* for secreted lignin peroxidases (LiPs), manganese peroxidases (MnPs), and H<sub>2</sub>O<sub>2</sub>-producing oxidases, which are thought to work together to cleave lignin into low-molecular-weight fragments (2). However, many aspects of ligninolysis by *P. chrysosporium* remain poorly understood.

First, uncertainty remains about the process of lignin depolymerization. White rot fungi remove lignin not only from the surface of the wood cell wall but also from its interior (3). Since the porosity of sound wood is too low for enzymes to infiltrate (3, 4), this observation suggests that the peroxidases do not cleave most of the lignin directly. Instead, low-molecular-weight oxidants that can enter the wood cell wall are likely involved. One possibility is that LiPs oxidize the secreted *P. chrysosporium* metabolite veratryl alcohol to produce diffusible, ligninolytic free radicals (2, 5). Alternatively, MnPs may oxidize fungal unsaturated fatty acids to produce reactive oxygen species (ROS) that oxidize lignin (6–8). A third possibility is that ligninolytic ROS may be produced via Fenton chemistry promoted by the enzyme cellobiose dehydrogenase

or by redox-active glycopeptides, both of which have been reported for *P. chrysosporium* (9–11).

Additionally, little is known about the subsequent steps that result in efficient mineralization of lignin. Since extracellular ligninolysis by fungal oxidants releases only a small proportion of the polymer's carbon as volatile products (12, 13), intracellular transport of the lignin fragments is presumably required, not only to enable catabolism but also to prevent the repolymerization of lignin oligomers under the prevailing oxidative conditions (14). Likewise, the export of the putative mediator veratryl alcohol and the import of its oxidation product veratraldehyde to permit reductive regeneration of veratryl alcohol may be key processes (15). The transporters and oxidoreductases responsible for this traffic in aromatic compounds have yet to be identified. Equally little is known about the intracellular metabolism of lignin fragments. Presumably, cytochrome P450 monooxygenases have an important role, because ring hydroxylation is required for breakdown of aromatic substrates (16), but an array of other, unidentified en-

Received 25 June 2015 Accepted 27 August 2015

Accepted manuscript posted online 4 September 2015

Citation Korripally P, Hunt CG, Houtman CJ, Jones DC, Kitin PJ, Cullen D, Hammel KE. 2015. Regulation of gene expression during the onset of ligninolytic oxidation by *Phanerochaete chrysosporium* on spruce wood. Appl Environ Microbiol 81:7802–7812. doi:10.1128/AEM.02064-15.

Editor: A. A. Brakhage

Address correspondence to Dan Cullen, dcullen@wisc.edu, or Kenneth E. Hammel, kehammel@wisc.edu.

Supplemental material for this article may be found at <http://dx.doi.org/10.1128/AEM.02064-15>

Copyright © 2015, American Society for Microbiology. All Rights Reserved.

zymes must also be involved. Moreover, little is known about the detoxification processes that protect the fungus from ligninolytic oxidants and the chemically reactive fragments they generate from lignin.

Although a definitive picture of the entire ligninolytic system in *P. chrysosporium* is not yet attainable, transcriptome analyses of the fungus grown on wood can provide useful clues. Initial work in this area employed quantitative reverse transcriptase PCR (RT-PCR) measurements of select transcripts and showed that ligninolytic peroxidases are highly expressed by *P. chrysosporium* on wood (17), but it did not address the overall coordination of lignin degradation. With the advent of the initial genome assembly and annotations (v1.0 and v2.1) (18), microarray-based transcriptome analysis allowed examination of transcript levels of *P. chrysosporium* genes during growth on ball-milled wood and in defined growth media (19–23). This approach provided useful insights but was limited to 10,048 v2.1 targets and complicated by the unpredictable manner in which the fungus responds to unnatural carbon sources in submerged basal salts medium. A complete, fully coordinated ligninolytic system may not be expressed by *P. chrysosporium* on ball-milled wood, because a potential route for regulatory feedback has been eliminated: the cellulose and hemicellulose in this substrate are readily accessible to enzymes (24), and thus, ligninolysis is not essential for growth.

An alternative approach is to compare levels of gene expression just before and after the onset of secondary metabolism and extracellular substrate oxidation by *P. chrysosporium* as it utilizes solid wood as its carbon source. If this can be done, and decay of the substrate is also confirmed, then the genes undergoing marked changes in expression during the metabolic transition can be identified with greater confidence. Although not all such genes are expected to have roles in biodegradation, this strategy may identify interesting candidates for future investigation. For this approach to work, a sensitive method is required to detect the production of extracellular oxidants by *P. chrysosporium* as wood decay commences. We have found that micrometer-scale fluorometric beads that react with ligninolytic oxidants are useful for this purpose (25). Here we report their use in conjunction with whole-transcriptome shotgun sequencing (RNA-seq) analysis to characterize changes in gene expression that occur during the transition to ligninolytic metabolism.

## MATERIALS AND METHODS

**Preparation of fluorometric oxidant-sensing beads.** The ratiometric oxidant-sensing dye BODIPY 581/591 was attached via amide linkages to porous silica beads functionalized with amino groups (Luna NH<sub>2</sub>, 3- $\mu$ m particle size; Phenomenex, Torrance, CA) as described previously (25), with the following modification: 312 nmol of BODIPY 581/591 succinimidyl ester (Life Technologies, Grand Island, NY) was first dissolved in 78  $\mu$ l of *N,N*-dimethylformamide and then added to 50 mg of beads that had been suspended beforehand in 1.4 ml of dry isopropanol. This procedure resulted in beads that were less oxidized than those prepared by our earlier method (25), as shown by the higher initial red/green ratio (RGR) of their fluorescence. The beads were calibrated with peroxyl radicals generated by the thermolysis of 2,2'-azobis(2-methylpropionamide) dihydrochloride (AAPH; Sigma-Aldrich, St. Louis, MO) as described previously (25). The calibration gave the following empirical relationship: millimolar concentration of radicals =  $(40 - 0.89\text{RGR})/\text{RGR}$ .

**Culture system.** *Phanerochaete* (= *Phanerochaetia*) *chrysosporium* (strain RP-78) was grown as described previously on microtomed tangen-

tial sections of spruce sapwood (*Picea glauca*, 40 mm long, 10 mm wide, 40  $\mu$ m thick, dry weight of approximately 7 mg) that were embedded on glass coverslips in 90  $\mu$ l of agar containing a nitrogen-mineral salts medium without nutrient carbon (25). For inoculation, conidiospores (10  $\mu$ l of a suspension containing approximately  $5 \times 10^6$  spores/ml) (26) and BODIPY beads (0.017 mg) were mixed with the warm liquid agar before the cultures were assembled as described earlier (25). The cultures were placed in sterile petri dishes and incubated under air at 38°C and 100% relative humidity.

Extents of BODIPY bead oxidation by the cultures were determined daily for 5 days by confocal fluorescence microscopy as described previously (25). On each day, five fields of view were randomly examined from each of three cultures to obtain data from a total of 15 fields (each 230  $\mu$ m<sup>2</sup>, 512 pixels wide). Their composite average RGR values (591 nm/581 nm fluorescence ratios) were recorded and converted to peroxyl radical equivalents using the calibration equation given above.

Extents of fungal growth in the cultures were estimated by measuring the total hyphal length in transmission images of the same fields as were examined to determine RGR values. Hyphae visible in the transmission channel were traced using the “draw freehand” tool provided in ImageJ software (available at <http://imagej.nih.gov/ij>), and the total length of all visible hyphae in the focal plane was summed using the ImageJ “measure” tool.

**Assessment of wood decay.** Harvested wood sections were rinsed for 5 min in water at 90°C to remove the agar. To assess incipient delignification by *P. chrysosporium* after 1 week using the safranin O/astra blue method (27), the fungus was grown on cross sections of spruce rather than tangential sections, but otherwise the culture system was identical to the usual procedure. The harvested sections were stained, destained, and observed by transmission microscopy as described previously (25). To assess decay after 8 weeks by scanning electron microscopy (SEM), colonized tangential wood sections were passed through a graded ethanol series, air dried, additionally dried in an oven overnight at 50°C, and mounted on specimen stubs. The sections were then sputter-coated with gold and observed with a Leo Evo-40 VP instrument operated at an accelerating voltage of 10 kV.

**Transcriptome analysis.** To obtain RNA for analysis, samples consisting of 20 colonized wood sections were harvested and pooled after 40 h and after 96 h. These pools were obtained in replicates at each time point as described below. The samples were immersed in liquid nitrogen and stored at –80°C until extraction. For total RNA purification, the wood was ground in a prechilled mortar and pestle in liquid nitrogen. Autoclaved and prechilled glass beads (0.5-mm diameter) were included during the grinding to reduce the wood to a fine powder. As described previously (23), following repeated phenol-chloroform extractions, RNA was ethanol precipitated at –20°C overnight and further purified using an RNeasy minikit (Qiagen, Valencia, CA). Total RNA was treated with DNase according to the manufacturer's protocol.

For RNA-seq analysis, total RNA was obtained as described above from three replicate pools of colonized wood sections at 40 h and at 96 h. Following verification of RNA purity and integrity using a NanoDrop spectrophotometer and Agilent 2100 BioAnalyzer, the Illumina TruSeq RNA protocol (Illumina Inc., San Diego, CA) was followed. mRNA was purified from 1  $\mu$ g of total RNA using poly(T) oligonucleotide-attached magnetic beads. Double-stranded cDNAs were synthesized using SuperScript II (Invitrogen, Carlsbad, CA) and random primers for first-strand cDNA synthesis, followed by second-strand synthesis using DNA polymerase I and then by RNase H treatment for removal of mRNA. Double-stranded cDNA was purified using Agencourt AMPure XP beads (Qiagen) as recommended in the TruSeq RNA sample prep guide. cDNAs were end repaired by T4 DNA polymerase and Klenow DNA polymerase and then phosphorylated with T4 polynucleotide kinase. The blunt-ended cDNA was purified using Agencourt AMPure XP beads. The cDNA products were incubated with Klenow DNA polymerase to add an adenine to the 3' end of the blunt phosphorylated DNA fragments and then purified using Agencourt AMPure XP beads. The DNA fragments were then ligated to

Illumina adapters having a single thymine overhang at their 3' ends. The adapter-ligated products were purified using Agencourt AMPure XP beads. Adapter-ligated DNA was amplified in a linker-mediated PCR (LM-PCR) for 15 cycles using Phusion DNA polymerase and Illumina's PE genomic DNA primer set and then purified using Agencourt AMPure XP beads. The quality and quantity of the finished libraries were assessed using an Agilent DNA1000 series chip assay (Agilent Technologies, Santa Clara, CA) and Invitrogen Qubit HS kit (Invitrogen), respectively, and the libraries were standardized to 2  $\mu$ M. Cluster generation was performed using a TruSeq Single Read Cluster kit (v3) and the Illumina cBot, with libraries multiplexed in a single HiSeq2000 lane. Images were analyzed using CASAVA v1.8.2, and FASTQ files were generated. DNASTar Inc. (Madison, WI) modules SeqNGen and Qseq were used for mapping reads and statistical analysis. The current Joint Genome Institute (JGI) annotation (v2.2), featuring 13,602 gene models, served as the queried database (<http://genome.jgi-psf.org/pages/dynamicOrganismDownload.jsf?organism=Phchr2>) (28). RNA-seq-based transcript results are presented as reads per kilobase per million (RPKM) values and are integrated with results from previously published v2.1 microarray studies in Data Set S1 in the supplemental material.

Twenty-three gene targets, most of them previously implicated in ligninolysis, were also selected for quantitative PCR analysis (RT-PCR). Total RNA, obtained as described above, was analyzed from four replicate pools of colonized wood sections at 40 h and at 96 h. Reverse transcription of the RNA was performed using oligo(dT) 18 primers from the Revert Aid H Minus first-strand cDNA synthesis kit (Life Technologies). RT-PCR analysis was performed using an ABI Prism7000 sequence detection system and SYBR green supermix with ROX reference dye (Bio-Rad, Hercules, CA). The reaction mixtures contained 10 ng of cDNA and 250 nM primers in a 20- $\mu$ l reaction volume. PCR amplification conditions were as follows: 2 min at 50°C, 10 min at 95°C, and then 40 cycles that consisted of 15 s at 95°C and 1 min at 58°C. The amplification reactions were shown to be target specific by obtaining dissociation curves over a temperature range of 60°C to 95°C. Gene-specific primers are listed in Table 1. Based on previous microarray results (23), the actin gene was selected as a suitable reference gene for computing cycle threshold ( $C_T$ ) ratios, which were compared to RNA-seq-derived RPKM values.

**Microarray data accession number.** Transcriptome data were deposited to the National Center for Biotechnology Information (NCBI) Gene Expression Omnibus (GEO) database (<http://www.ncbi.nlm.nih.gov/geo/>) and assigned accession no. GSE69461.

## RESULTS AND DISCUSSION

**Fungal growth and wood decay.** We grew *P. chrysosporium* using thin sections of spruce wood as the carbon source. The sections, placed on coverslips, were embedded in mineral salts agar that contained a dispersion of conidiospores as the inoculum (see Fig. S1A in the supplemental material). Figure 1A shows the typical appearance of a day 2 culture as observed by transmission microscopy through the coverslip, and Fig. 2A shows the total hyphal length per microscopic field of view, in a plane immediately above the wood surface, for each day in culture. The data points represent averages from 15 analyzed images for each day. By day 2, the total hyphal length reached a value that was not significantly different from the values for days 3 to 5. The hyphal length for day 1 was about 50% of the apparent final value and was statistically different from the data for subsequent days ( $P \leq 0.013$  by pairwise  $t$  tests). These results indicate that fungal growth ceased after 2 days. Staining of the inoculated wood with safranin/astra blue after 1 week of colonization showed an increased blue color characteristic of incipient delignification (see Fig. S2A and B) (27), which indicated that the cultures were biodegradatively competent. Scanning electron microscopy after 8 weeks confirmed this

result, showing extensive, erosive decay of the substrate (see Fig. S2C and D).

**Onset of extracellular oxidation.** Also included in the agar and sandwiched against the wood of these cultures were oxidant-sensing fluorometric beads based on the covalently attached dye BODIPY 581/591 (see Fig. S1B). Since the dye is immobilized, it is susceptible only to extracellular oxidants, a wide variety of which have been shown to oxidize it (25, 29). As described in detail elsewhere (25), detection of oxidation is performed by confocal fluorescence microscopy through the coverslip: native beads fluoresce red, whereas oxidized beads fluoresce green.

Figure 1B and C show the typical appearance of the beads on days 2 and 4, respectively. Figure 2 shows that little oxidation occurred on days 1 and 2, whereas by day 5, the beads were fully oxidized. For days 3 and 4, all of the beads in most fields of view were fully oxidized, but in some fields none of the beads were oxidized. This clustering indicates that the onset of oxidation was not completely synchronous across the wood. Few images showed intermediate levels of oxidation, likely because the relatively small amount of dye available on the beads became quickly saturated with oxidants as biodegradation commenced. That is, the beads essentially functioned in our experiments as binary ("off" or "on") indicators of when oxidation commenced. Consequently, the oxidation data for any particular day cannot be well expressed as an arithmetic average.

Therefore, we present the data as the percentage of images exhibiting an oxidation level greater or less than that given when uninoculated cultures were treated with a 10 mM concentration of our calibration oxidant, AAPH. This is the level of oxidation that distinguishes most cleanly between oxidized and nonoxidized images. Our analysis shows that no images exhibited significant oxidation on day 1 or 2, whereas by days 3 and 4, 70% to 80% of the inspected fields were oxidized. Finally, on day 5, all fields were oxidized (Fig. 2). These results establish that the onset of oxidation in the colonized wood occurred between days 2 and 3. Comparison of the time courses for hyphal elongation and bead oxidation indicates that the hyphae stopped growing after 2 days and only then began to oxidize their surroundings (Fig. 2A), which is consistent with extracellular oxidation being a function of secondary metabolism.

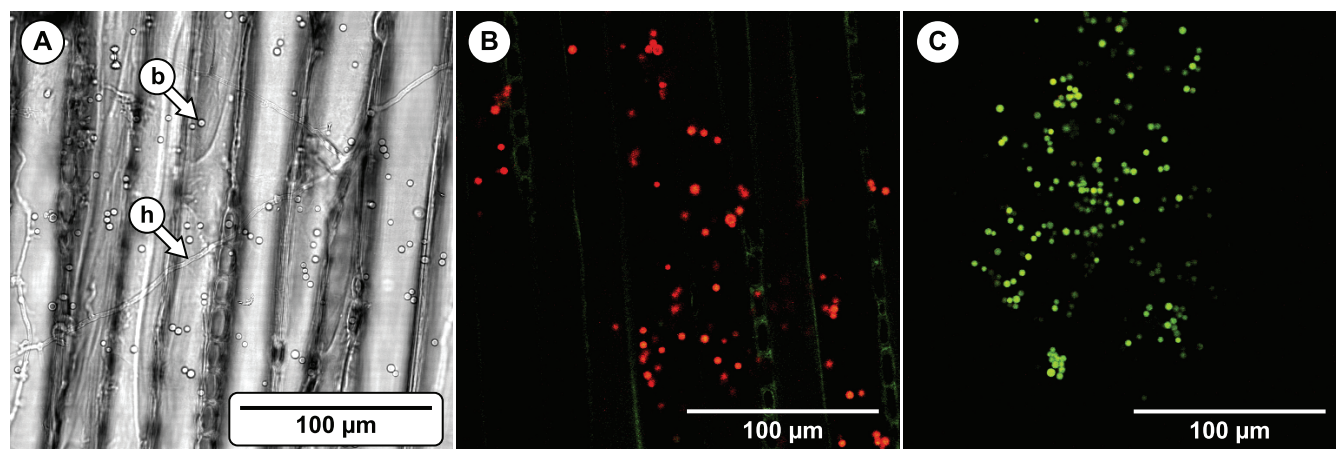
**Transcript profiles.** We extracted RNA from triplicate pools of cultures harvested at 40 h and at 96 h. The two times selected bracket the onset of extracellular oxidation. The 40-h and 96-h samples provided, in total,  $2.5 \times 10^8$  and  $1.6 \times 10^8$  RNA-seq reads, respectively, and these were mapped to the most recent (v2.2) *P. chrysosporium* genome (see Data Set S1 in the supplemental material). Each of the six samples had more than  $5.2 \times 10^7$  assigned reads, ample coverage for confident statistical analyses. Of the 13,602 models, transcripts corresponding to 431 genes were at least 4-fold more abundant at 96 h than at 40 h ( $P < 0.01$ ), and transcripts corresponding to 451 genes were at least 4-fold more abundant at 40 h than at 96 h ( $P < 0.01$ ). Considering only those transcripts with relatively high RPKM values ( $>10$ ) at 96 h, 356 were significantly more abundant relative to the numbers found at 40 h (Fig. 3). For brevity, we arbitrarily refer to these genes as upregulated. Applying the same threshold, 252 genes were more highly expressed in 40-h samples than in 96-h samples and thus appear downregulated (Fig. 3). Focusing on a subset of gene targets that already have proposed ligninolytic roles, we found that RNA-seq comparisons with quantitative RT-PCR showed good

TABLE 1 Primers used for quantitative PCR analysis

Model ID (v2.1)/gene <sup>a</sup>	Primer	Primer sequence	Length (bp)
10957/LiPA	LipAF	5'GAAGCCATTTCGTTTCTCAGAACG3'	20
	LipAR	5'TCGTTGACACGGTTGATGAT3'	20
121822/LiPB	LipBF	5'CGTGTTCACGATGCTATT3'	19
	LipBR	5'CGGCTTCTGGAGGTTGATAA3'	20
131738/LiPC	LipCF	5'GCTCCTTGCTGTCTTACCG3'	20
	LipCR	5'ATCGGACAGAACGTTGAACC3'	20
68111/LiPD	LipDF	5'TTCGACTCCCAGTTCTTCGT3'	20
	LipDR	5'CAGCTTCGTCTGGTTGTTGA3'	20
11110/LiPE	LipEF	5'GAGCTCGTCTGGATGCTTTC3'	20
	LipER	5'AGTGCCACGGAAGTCTGCT3'	20
122202/LiPF	LipFF	5'CAACCAGGGTGAGGTTGAAT3'	20
	LipFR	5'ACGAGCTTCGACTGGTTGTT3'	20
8895/LiPG	LipGF	5'GACGACATCCAGCAGAACCT3'	20
	LipGR	5'GATAGAGCCGTCAGCACCTC3'	20
121806/LiPH	LipHF	5'ATGGCTTTCAAGCAACTCGT3'	20
	LipHR	5'TGTCGTCGAGAACATCGAAC3'	20
131707/LiPI	LipIF	5'TCATCAGCCGTGTCAATGAT3'	20
	LipIR	5'CGAAGAACTGGGAGTCAAG3'	20
131709/LiPJ	LipJF	5'TTTGTGAGACACAGCTTGC3'	20
	LipJR	5'GAGCTTCGACTGGTTGTTG3'	19
8191/MnP1	Mnp1F	5'AGGTCATCCGTCTGACGTTTC3'	20
	Mnp1R	5'AGGTCATCCGTCTGACGTTTC3'	20
3589/MnP2	Mnp2F	5'AGACAGCGTCACCAAAATCC3'	20
	Mnp2R	5'GTGTCGAAGGTGAAGGGTGT3'	20
878/MnP3	Mnp3F	5'TTCGCCTTACTTTCCACGAC3'	20
	Mnp3R	5'AGAAGTTGGGCTCAATGGTG3'	20
4636/MnP4	Mnp4F	5'CCACAGTCGTAGCAACCTGA3'	20
	Mnp4R	5'GTTTCGAGCAGTGGGGAATAA3'	20
140708/MnP5	Mnp5F	5'TACCGTTCATGCAGAAGCAC3'	20
	Mnp5R	5'AGGATCTTGGTCACGCTGTC3'	20
1923/glycopeptide 1	Glp1F	5'GTCAGCTTCGCAAACTG3'	20
	Glp1R	5'GGAGAACGCATGCCTAGAAC3'	20
1926/glycopeptide 2	Glp2F	5'GCTATCGCTTTCTGTCAGAC3'	20
	Glp2R	5'CGTAGTACCCGAAGCCAGAG3'	20
11068/glyoxal oxidase	GloxF	5'TCACACCTTCGCTCTACACG3'	20
	GloxR	5'ATGAAGAAGTTGCCCTGCTG3'	20
11098/cellobiose dehydrogenase	CdhF	5'GTGCTTCTCCCAAGCTCAAC3'	20
	CdhR	5'GACTGGATGCCCGTAGAGAG3'	20
126879/alcohol oxidase	AoxF	5'ATCCGCTGGAGCTACAAGAA3'	20
	AoxR	5'ATCTGCTTGGCAGTCTCGAT3'	20
124439/phenylalanine ammonia lyase	PalF	5'TCAAGGCTGAGGACGAAGTT3'	20
	PalR	5'TCAAGAGTGACCGTCTCTGTG3'	20
124398/catalase	CatF	5'TGCAGTCCCGTCTCTTCTCT3'	20
	CatR	5'GGACGAGCGAACTCTGGTAG3'	20
139298/actin	AcF	5'GCATGTGCAAGGCTGGCTTTG3'	21
	AcR	5'AGGGCGACCAACGATGGATG3'	20

<sup>a</sup> Primers were designed based on the v2.1 database, as v2.2 was not yet available.





**FIG 1** (A) Transmission micrograph of a day 2 culture showing *P. chrysosporium* hyphae (h) and BODIPY beads (b). (B) Confocal fluorescence micrograph showing red BODIPY beads in a day 2 culture. The faint green lines in the background are due to autofluorescence of the wood. (C) Confocal fluorescence micrograph showing green BODIPY beads in a day 4 culture.

agreement for the two methods (see Fig. S3 in the supplemental material). Among the RNA-seq data, the following transcripts, categorized according to their proposed roles, stand out for discussion.

**Ligninolysis by peroxidases.** Transcripts of six genes encoding LiPs (Phach protein identifiers [ID] 1386770, 1716042, 1716776,

2918435, 2989894, and 3032409) were markedly elevated after the onset of extracellular oxidation in the cultures (Table 2). Interestingly, the relative transcript levels for *lipD*, *lipE*, *lipB*, and *lipA* were generally similar at 96 h to the pattern seen in carbon-limited glucose liquid medium (30). Our culture system was stoichiometrically nitrogen limited (ca. 600 µmol of C versus 0.2 µmol of N per culture), but the low bioavailability of wood polysaccharides as a carbon source may have produced a *de facto* carbon limitation. Transcripts encoding three MnPs (Phach ID 3589, 8191, and 2971944) were also much more abundant at 96 h than at 40 h. In addition, transcripts encoding some enzymes that are proposed to

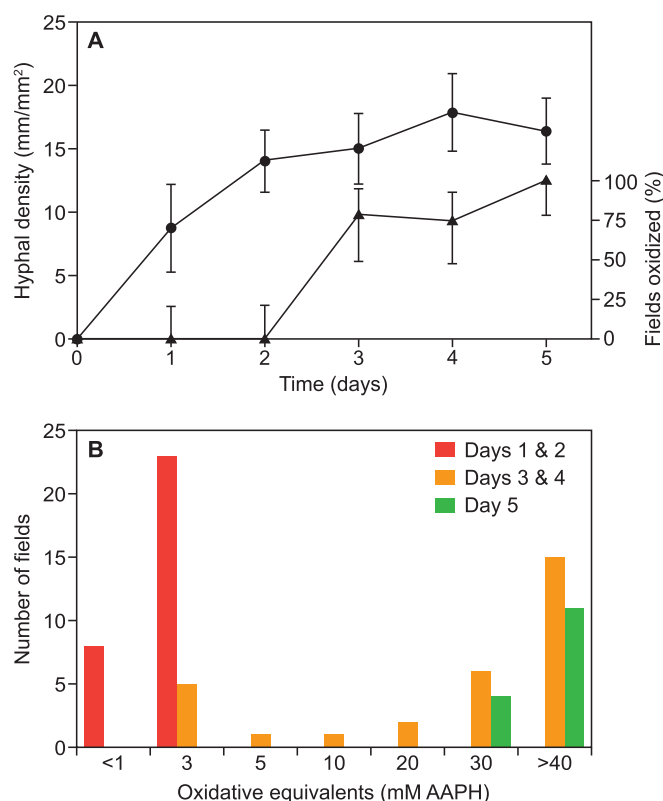


**FIG 2** (A) Time courses of fungal growth (hyphal density, circles) and BODIPY bead oxidation (percentage of microscopic fields oxidized, triangles) on colonized wood sections. The error bars show 95% confidence intervals. (B) Histogram showing distributions of BODIPY bead oxidation in wood samples colonized for 1 or 2 days, 3 or 4 days, and 5 days.

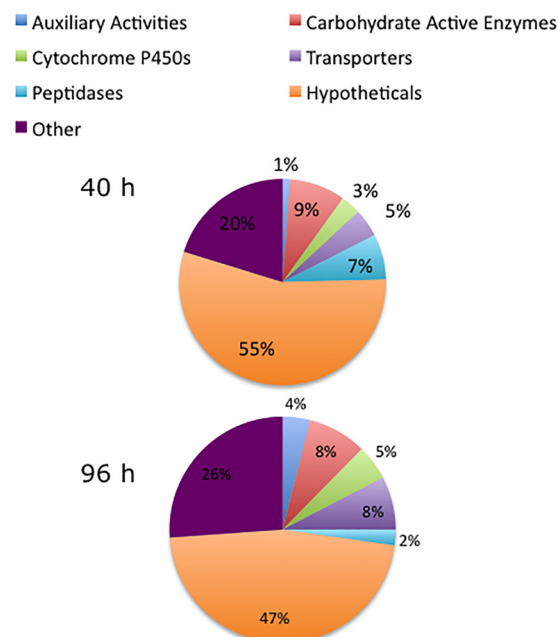


**FIG 3** Classification and distribution of genes upregulated (more than 4-fold;  $P < 0.01$ ) in colonized wood after 40 h relative to 96 h (upper chart) and at 96 h relative to 40 h (lower chart). Genes with RPKM values less than 10 were excluded, leaving data sets of 252 genes and 356 genes for 40 h and 96 h, respectively.

**TABLE 2** Transcripts of genes implicated in lignin degradation showing more than 4-fold accumulation after 96 h

Model ID <sup>a</sup>		RPKM (log <sub>2</sub> ) <sup>b</sup>		Putative function	Comment(s) <sup>c</sup>	Ratio, <sup>d</sup> 96 h/40 h
v2.2	v2.1	96 h	40 h			
1386770	6811	11.69	2.87	Peroxidase LiPD	AA2; SS	450.80
1716042	11110	12.64	4.02	Peroxidase LiPE	AA2; SS	394.25
2971944	140708	12.15	3.97	Peroxidase MnP1	AA2; SS	290.91
8191	8191	12.40	4.38	Peroxidase MnP4	AA2; SS	258.50
1716776	121822	9.41	1.62	Peroxidase LiPB	AA2; SS	220.23
11068	11068	11.89	4.39	Glyoxal oxidase	AA5_1; SS	181.30
3589	3589	10.37	3.37	Peroxidase MnP2	AA2:SS	128.52
2661209	4969	9.58	3.35	O-Methyltransferase		75.23
2907675	136354	7.49	1.29	Oxalate decarboxylase	SS	73.89
2989894	10957	7.53	1.89	Peroxidase LiPA	AA2:SS	50.06
3004321	126879	12.71	7.08	Alcohol oxidase (methanol oxidase)	AA3_3	49.26
2918435	8895	8.67	3.05	Peroxidase LiPG	AA2; SS	49.17
2974896	987	9.47	4.16	O-Methyltransferase		39.68
1677212	140586	6.86	1.75	Aldehyde reductase	Aldo/keto reductase	34.50
2971127	124439	9.28	4.79	Phenylalanine ammonia lyase	Cinnamate synthesis	22.44
2987995	2988210	6.58	2.31	Formaldehyde dehydrogenase		19.20
3032409	131738	6.82	2.57	Peroxidase LiPC	AA2; SS	19.02
3005740	None	8.13	4.22	Phenol hydroxylase	Monooxygenase	15.05
2903766	None	8.25	4.66	GST <sup>e</sup>	GST family	12.00
11055	11055	9.43	5.96	Aryl alcohol dehydrogenase	Aldo/keto reductase	11.08
3023907	None	7.35	3.91	O-Methyltransferase		10.81
2934397	122129	8.19	4.76	Lytic polysaccharide monooxygenase	AA9	10.78
3031669	140211	12.10	8.74	Formate dehydrogenase		10.25
2971108	7168	7.78	4.75	GST	GST family	8.17
2897793	139901	4.80	2.06	Benzoquinone oxidoreductase	AA6	6.68
1961248	9193	7.83	5.14	O-Methyltransferase		6.44
2979948	3858	8.30	5.62	Aldehyde dehydrogenase	NAD(P) dependent	6.41
1036159	191	7.26	4.63	Prephenate dehydrogenase	Tyr synthesis	6.21
2990377	9194	5.99	3.54	O-Methyltransferase		5.44
3028048	138696	7.16	4.77	Aryl alcohol dehydrogenase	Aldo/keto reductase	5.26
3006241	3006456	12.32	10.25	Catalase		4.20
137014	137014	10.71	8.34	Aldehyde dehydrogenase	NAD(P) dependent	5.17
2983773	5406	4.02	1.97	Multicopper oxidase MCO2	AA1	4.16
2922705	41330	9.00	6.98	Aromatic compound dioxygenase	Dioxygenase	4.06

<sup>a</sup> Protein models corresponding to v2.1 and v2.2 (<http://genome.jgi-psf.org/Phchr2/Phchr2.home.html>).<sup>b</sup> RPKM, reads per kilobase per million.<sup>c</sup> AA, auxiliary activities as defined by Levasseur et al. (50); SS, secretion signal. Genes encoding LiPE, LiPB, LiPA, LiPG, and LiPC are clustered within a 100-kb region (30). Close linkage (<5 kb) was not observed among the other listed genes.<sup>d</sup> All ratios with *P* values of <0.001.<sup>e</sup> GST, glutathione S-transferase.

support LiP and MnP turnover were significantly higher at 96 h. These include the copper radical oxidase, glyoxal oxidase (Phach ID 11068), and the GMC oxidoreductase, methanol oxidase (Phach ID 3004321), which are generally thought to generate some of the extracellular H<sub>2</sub>O<sub>2</sub> required by LiPs and MnPs (31).

Also elevated was the transcript for phenylalanine ammonia lyase (Phach ID 2971127), which catalyzes the first step in the biosynthesis of veratryl alcohol (32, 33), a secreted aromatic co-factor thought to promote ligninolysis by LiPs (2). O-Methyltransferases are also likely required to introduce the two ring methoxyl groups in veratryl alcohol (34), and five genes encoding them were upregulated (Phach ID 2974896, 1961248, 2661209, 2990377, and 3023907), although their specific biosynthetic roles remain to be determined. Veratryl alcohol levels may additionally be maintained in a salvage reaction via reductive recycling of the veratraldehyde produced when LiPs oxidize the alcohol. This reaction is likely catalyzed by intracellular aryl alcohol dehydroge-

nases (15), two of which were upregulated at the transcript level (Phach ID 11055 and 3028048).

In addition, enzymes involved in the biosynthesis of linoleic acid, the major membrane fatty acid in *P. chrysosporium* and other white rot basidiomycetes (35), are potentially relevant, because linoleic acid and other unsaturated lipids are oxidized by MnPs *in vitro* to produce ligninolytic oxidants (8, 36–38). Some transcripts encoding Δ<sup>9</sup> fatty acid desaturases were moderately more abundant at 96 h, notably Phach ID 1783939 (see Table S1 in the supplemental material). The gene for the single known *P. chrysosporium* Δ<sup>12</sup> desaturase (Phach ID 3007445), also presumably required for linoleate production (39), was not upregulated. However, its transcript had the highest RPKM value among the fatty acid desaturases.

**Ligninolytic ROS metabolism.** Both H<sub>2</sub>O<sub>2</sub> and Fe<sup>2+</sup> are required components for a ligninolytic Fenton system (40). On one hand, transcripts for H<sub>2</sub>O<sub>2</sub>-producing oxidases were more abun-

TABLE 3 Transcripts of genes classified as CAZys showing more than 4-fold accumulation after 96 h<sup>a</sup>

Model ID <sup>b</sup>		RPKM (log <sub>2</sub> ) <sup>c</sup>		Putative classification	Comment(s) <sup>d</sup>	Ratio, <sup>e</sup> 96 h/40 h
v2.2	v2.1	96 h	40 h			
2983729	138715	9.40	1.80	GH10, <i>xyn10B</i> , endo-1,4-β-xylanase	CBM1; SS	194.17
2935636	125669	10.05	2.87	GH10, <i>xyn10D</i>	SS	145.23
3038104*		7.91	1.30	CE16	SS	97.48
2934294	132137	6.21	0.76	CE8	SS	43.79
2967379	128479	9.16	4.17	EXPN	SS	31.69
3042040	7852	8.35	3.89	GH10, <i>xyn10F</i> endo-1,4-β-xylanase	SS	22.05
2910342	132266	8.01	3.97	GH115	SS	16.45
2912243	6482	9.22	5.23	CE15, glucuronyl esterase	SS	15.80
2918600	8908	5.12	1.23	GT8 fragment		14.81
2934334	122292	7.94	4.22	GH78	SS	13.13
3004047*		8.24	4.94	CE16	SS	9.86
1521209	135606	7.97	4.77	GH131 fragment	SS	9.22
3037385	3651	9.33	6.23	GH51, <i>arb51A</i> α-N-arabinofuranosidase	SS	8.61
2896433	333	6.94	4.08	GH43, possible xylosidase/arabinosidase	SS	7.22
3031733		6.90	4.08	GH79	SS	7.05
2919526	9257	8.08	5.26	GH3, possible β-xylosidase	SS	7.02
2989563		6.56	3.81	GH28, exopolygalacturonase	SS	6.71
3006885	8072	10.16	7.45	GH55, <i>exg55A</i> glucan 1,3-β-glucosidase	SS	6.58
2979830	3795	6.81	4.14	GH28, exopolygalacturonase	SS	6.39
3027410	4449	8.23	5.58	GH28, <i>epg28B</i>	SS	6.30
3010808	134001	4.92	2.29	GH27, α-galactosidase	CBM1; SS	6.20
2904202	3805	10.05	7.55	GH28, <i>epg28A</i> polygalacturonase	SS	5.66
2898396	1999	6.11	3.66	GH79	SS	5.49
2989297	8580	5.64	3.26	CE8	SS	5.21
2983356	138710	6.77	4.49	GH53, endo-1,4-β-galactosidase	SS	4.87
3004260		6.13	4.04	GH79	SS	4.25
3023377	139777	7.01	4.94	GH125	SS	4.19
2552	2552	9.80	7.78	CBM13		4.07
2661256	4971	8.73	6.70	GH13_40, α-1,6-glucosidase		4.06
3024004	139732	7.51	5.49	GH10, endo-1,4-β-xylanase	CBM1; SS	4.06

<sup>a</sup> CAZys (<http://www.cazy.org>) assigned to families of glycoside hydrolases (GH), carbohydrate esterases (CE), glycosyltransferases (GT), carbohydrate binding modules (CBM), or expansins (EXPN).  
<sup>b</sup> Protein models corresponding to v2.1 and v2.2 (<http://genome.jgi-psf.org/Phchr2/Phchr2.home.html>). Asterisks indicate the only closely linked (<5 kb) gene models.  
<sup>c</sup> RPKM, reads per kilobase per million.  
<sup>d</sup> CBM1, carbohydrate binding domain family 1; SS, secretion signal.  
<sup>e</sup> Ratios all with *P* values of <0.001.

dant after the onset of extracellular oxidation, as outlined above (Table 2). On the other hand, transcripts encoding proteins with proposed roles in Fe<sup>3+</sup> reduction (cellobiose dehydrogenase, Phach ID 3030424) (9) or Fe<sup>2+</sup> chelation (redox-active glycopeptides, Phach ID 3023982 and 3023986) (10) were not upregulated. However, it should be noted that emphasis on upregulation, *per se*, does not necessarily capture the physiological roles of degradative proteins expressed. The high RPKM value of 1,358 for cellobiose dehydrogenase at 96 h appears consistent with a biodegradative role, even though the RPKM value was slightly higher at 40 h. For perspective, only 0.6% of the 13,602 gene models had RPKM levels greater than 1,000. The very low RPKM values below 5 found for the glycopeptides at 96 h call into question their proposed roles in the production of ligninolytic hydroxyl radicals.

Some other genes with proposed involvement in production of ROS or protection from them were also upregulated at 96 h. Transcripts were elevated for a catalase (Phach ID 3006241) and the multicopper oxidase MCO2 (Table 2). The latter enzyme may oxidize Fe<sup>2+</sup>, since the closely related ferroxidase MCO1 has this activity (41). H<sub>2</sub>O<sub>2</sub> depletion and Fe<sup>2+</sup> oxidation by these routes may have a role in modulating Fenton chemistry, which not only

targets lignocellulose but also is potentially destructive to the fungal mycelium. In addition, we observed upregulation of an oxalate decarboxylase gene (Phach ID 2907675), which could have a role in modulating levels of oxalate. This dicarboxylic acid has a likely role in ROS production because it is the principal chelator of Fe<sup>3+</sup> in many wood decay basidiomycetes (25). Also elevated was the transcript for an intracellular benzoquinone reductase (Phach ID 2897793), which might generate Fenton reagent by catalyzing quinone redox cycling in the presence of Fe<sup>3+</sup> (42). However, it should be noted that white rot fungi have not been found to produce the requisite benzoquinones, in contrast to the brown rot fungi, which have been shown to employ this mechanism (43). It appears more likely that the *P. chrysosporium* benzoquinone reductases have a role in detoxifying quinones derived from the fungal catabolism of low-molecular-weight lignin fragments (44). Although their substrate preferences are poorly understood, upregulated genes encoding glutathione S-transferases (Phach ID 2903766 and 2971108) and aldehyde dehydrogenases (Phach ID 2979948 and 137014) also have a likely role in intracellular detoxification (45).

**Transport and catabolism of lignin fragments.** The particular transporters and cytochrome P450s involved in lignin degrada-

**TABLE 4** Genes encoding hypothetical proteins with secretion signals and showing more than 4-fold transcript accumulation at 96 h relative to 40 h<sup>a</sup>

Model ID		v2.2 gene location, scaffold:coordinates	Comment, v2.2	RPKM (log <sub>2</sub> ) <sup>b</sup>		Ratio, 96 h/40 h	Related gene(s) <sup>c</sup>
v2.2	v2.1			96 h	40 h		
2393773	None	6:273742–274727	3037881 preferred	4.78	1.84	97.81	3026500
1911099	1903	2:2691027–2692451	SS	9.16	3.47	51.45	None
2870733	6097	10:667148–667591	SS	7.99	2.45	46.40	≥5; e.g., 2919481
3026500	None	6:277446–278353		7.92	2.46	43.86	2393773
2985926	6581	11:766956–768138	3055967 linked	6.59	1.91	25.66	None
3570	3570	5:458757–459429		8.08	3.40	25.60	None
2919481	9262	23:74536–75162		7.20	2.59	24.46	≥5; e.g., 2870733
3034369	612	1:1896580–1898032	TMH	11.60	7.33	19.35	611
3019728	6895	12:214502–216334		4.58	0.72	14.61	None
2198003	None	4:964949–965506		6.45	2.86	12.09	None
3026785	None	6:1087020–1087477		8.51	5.05	11.02	None
2959275	6854	12:100059–100918		7.88	5.16	6.59	2913810
2894568	280	1:865111–867528		7.09	4.71	5.19	3001131
3055967	6583	11:770265–771840	2985926 linked	3.67	1.64	4.07	None

<sup>a</sup> v2.1 model ID 1903, but not the corresponding v2.2 model, has extended 5' terminus with secretion signal. Abbreviations: SS, secretion signal; TMH, transmembrane helix.

<sup>b</sup> RPKM, reads per kilobase per million.

<sup>c</sup> Related sequences with e-values of  $<10^{-50}$  and/or bit scores of  $>500$ . Model ID 611 is upregulated 3.1-fold (see Data Set S1 in the supplemental material) and lies adjacent to ID 3034369.

tion remain unknown, but our results identify candidates for future investigation: genes encoding 27 putative transporters (see Table S3 in the supplemental material) and 18 cytochrome P450s (see Table S4) (46, 47) were upregulated, in some cases with high RPKM values, at the onset of extracellular oxidation. An additional potential contributor to lignin fragment metabolism is the upregulated gene encoding protein Phach ID 2922705 (Table 2). Related to known catechol 1,2-dioxygenases (e.g., 41% identical to the *Rhodococcus opacus* enzyme [GenBank accession no. Q6F4M7.1]), this enzyme may be involved in ring cleavage of aromatic metabolites. High transcript levels and upregulation were also noted for genes encoding the putative formaldehyde dehydrogenases Phach ID 2975262 and 2987995 and the formate dehydrogenase Phach ID 3031669. These enzymes may operate together with the aforementioned *P. chrysosporium* methanol oxidase (Phach ID 3004321) in the metabolism of methanol derived from lignin methoxyl groups.

**Polysaccharide degradation.** Of 175 glycoside hydrolase (GH) gene models in the *P. chrysosporium* genome, only 23 were associated with more than 4-fold transcript accumulation after the onset of extracellular oxidation (Table 3). Most of these putative carbohydrate-active enzymes (CAZys) are defined as hemicellulases (48, 49) and likely operate in conjunction with carbohydrate esterases (CE), several of whose gene transcripts were also upregulated. Again, we note that the degree of upregulation does not tell the whole story. For example, the GH10 gene *xyn10B* (Phach ID 2983729) is the most highly regulated GH-encoding gene, but on the basis of the transcript levels at 96 h, 14 other GHs may be more abundant (see Data Set S1 in the supplemental material). Thus, transcripts encoding the well-known cellobiohydrolases CBH1 (*cel7F* [Phach ID 2976248] and *cel7D* [Phach ID 137372]) and CBH2 (*cel6* [Phach ID 2965119]) were only 2.5-, 3.9-, and 2.3-fold more abundant, respectively, after 96 h, considerably less than the 194-fold recorded for *xyn10B* (Table 3). However, the normalized RPKM values at 96 h were 4,933, 4,662, and 2,165 for *cel7F*, *cel6* and *cel7D*, respectively (see Data Set S1), which are much higher than the values for most gene models, as noted above, and also higher than the value of 675 for *xyn10B*. An endo-1,4- $\beta$ -glucanase

gene classified as *cel5B* (Phach ID 2981757) was also highly expressed (3,284 RPKM) but exhibited only modest transcript accumulation at 96 h relative to 40 h (1.5-fold).

One of 16 *P. chrysosporium* genes encoding a lytic polysaccharide monooxygenase (LPMO) was upregulated more than 4-fold at 96 h. Formerly classified as glycoside hydrolases (50), these enzymes are now known for their oxidative attack on cellulose and xylans (51–55). The current protein model for the upregulated LPMO (Phach ID 2934397) lacks a secretion signal, but the alternative model given for it in the v2.1 database (Phach ID122129) features a complete N terminus with a predicted secretion signal. Beyond this gene, five additional LPMO-encoding genes were upregulated more than 2-fold, and three of these were highly expressed, with RPKM values greater than 2,000, at 96 h (see Data Set S1).

**Uncharacterized components of secondary metabolism.** Transcripts corresponding to 165 genes tentatively identified as hypotheticals accumulated more than 4-fold ( $P < 0.01$ ) in 96-h samples relative to 40-h samples (see Data Set S1). Of these, 14 had predicted secretion signals (Table 4). Eight showed no significant similarity to any NCBI and/or JGI sequences, although putative *P. chrysosporium* paralogs were detected in some instances. For example, the highly expressed gene encoding Phach ID 3034369 was closely linked on the same scaffold to Phach ID 611, a putative paralog upregulated 3.1-fold in 96-h samples. These genes feature a cupredoxin domain and a 3' transmembrane helix (TMH), suggesting possible involvement in electron transport. Phach ID 3034369 is closely related ( $e < 10^{-50}$  and/or bit scores  $> 500$ ) to sequences in the genomes of the white rot fungi *Phlebiopsis gigantea*, *Bjerkandera adusta*, *Exidia glandulosa*, and *Cerrena unicolor* and also to a sequence in the ectomycorrhiza-forming gasteromycete *Scleroderma citrinum* (56).

**Conclusions.** Our results support a ligninolytic role in *P. chrysosporium* for LiPs, MnPs, and some of the auxiliary enzymes that have been proposed to support their activity. Nevertheless, it is important to note that questions remain regarding the specific roles of the peroxidases. Thus far, they have not been shown to delignify natural lignocellulose, as opposed to the synthetic model



substrates that are generally used to assay them (2). The possibility must still be considered that the peroxidases function principally in the cleavage of soluble lignin oligomers produced by the action of other oxidants on the wood cell wall. These other agents could be ROS produced via Fenton chemistry or lipid peroxidation (40). Our data are consistent with roles for cellobiose dehydrogenase or MnPs in ligninolytic ROS generation but do not support a role for iron-chelating glycopeptides.

Our results also show that the transition to secondary metabolism and extracellular oxidant production in *P. chrysosporium* was not accompanied by a general upregulation of enzymes involved in cellulose hydrolysis. The high RPKM values we found for some of these glycoside hydrolases may indicate that they are expressed constitutively during incipient wood decay. A constitutive expression of cellulases would be consistent with the simultaneous decay pattern, as opposed to selective delignification, that is generally observed for *P. chrysosporium* (38). The high level of expression we found for cellulolytic genes could also indicate a functional carbon limitation when wood is the carbon source, although it must be noted that the data supporting this view were obtained using submerged liquid cultures of *P. chrysosporium* (23). In any case, our results do not rule out the possibility that cellulases may be upregulated at a later stage of decay, when sufficient lignin has been removed for them to infiltrate the wood cell wall. Additional time course experiments, conducted over longer intervals, will be required to answer these questions.

Finally, transcriptomics in combination with functional analysis of extracellular oxidation has proven to be a useful approach. In conjunction with the new v2.2 database for the *P. chrysosporium* genome, these experiments have identified a subset of potentially relevant proteins whose transcripts were upregulated at the onset of ligninolytic metabolism. These include not only enzymes that already had proposed roles but also transporters, cytochrome P450 monooxygenases, and proteins with no currently assigned function. With regard to this last category, the new database provides some new protein models that were not present in the v2.1 database: 72 of the genes we found to be upregulated at 96 h fall into this group. These new identifications will hopefully provide researchers with foci for further work on fungal ligninolysis.

## ACKNOWLEDGMENTS

We are grateful to Sandra Splinter BonDurant and Marie Adams of the University of Wisconsin Biotechnology Center for RNA processing and DNA sequencing, respectively, to Michael D. Mozuch of the U.S. Forest Products Laboratory for additional technical contributions, and to Robert Riley of the Joint Genome Institute for cross-listing the v2.1 and v2.2 protein models.

This work was supported by grant DE-SC0006929 (K.E.H., C.G.H., and C.J.H.) from the U.S. Department of Energy, Office of Biological and Environmental Research.

## REFERENCES

- Kirk TK, Farrell RL. 1987. Enzymatic "combustion": the microbial degradation of lignin. *Annu Rev Microbiol* 41:465–505. <http://dx.doi.org/10.1146/annurev.mi.41.100187.002341>.
- Hammel KE, Cullen D. 2008. Role of fungal peroxidases in biological ligninolysis. *Curr Opin Plant Biol* 11:349–355. <http://dx.doi.org/10.1016/j.pbi.2008.02.003>.
- Blanchette R, Krueger E, Haight J, Akhtar M, Akin D. 1997. Cell wall alterations in loblolly pine wood decayed by the white-rot fungus, *Ceriporiopsis subvermispora*. *J Biotechnol* 53:203–213. [http://dx.doi.org/10.1016/S0168-1656\(97\)01674-X](http://dx.doi.org/10.1016/S0168-1656(97)01674-X).
- Flournoy D, Paul J, Kirk TK, Highley T. 1993. Changes in the size and volume of pore in sweet gum wood during simultaneous rot by *Phanerochaete chrysosporium*. *Holzforschung* 47:297–301. <http://dx.doi.org/10.1515/hfsg.1993.47.4.297>.
- Candeias LP, Harvey PJ. 1995. Lifetime and reactivity of the veratryl alcohol radical cation. Implications for lignin peroxidase catalysis. *J Biol Chem* 270:16745–16748.
- Bao W, Fukushima Y, Jensen KA, Jr, Moen MA, Hammel KE. 1994. Oxidative degradation of non-phenolic lignin during lipid peroxidation by fungal manganese peroxidase. *FEBS Lett* 354:297–300. [http://dx.doi.org/10.1016/0014-5793\(94\)01146-X](http://dx.doi.org/10.1016/0014-5793(94)01146-X).
- Enoki M, Watanabe T, Nakagame S, Koller K, Messner K, Honda Y, Kuwahara M. 1999. Extracellular lipid peroxidation of selective white-rot fungus, *Ceriporiopsis subvermispora*. *FEMS Microbiol Lett* 180:205–211. <http://dx.doi.org/10.1111/j.1574-6968.1999.tb08797.x>.
- Kapich AN, Jensen KA, Hammel KE. 1999. Peroxyl radicals are potential agents of lignin biodegradation. *FEBS Lett* 461:115–119. [http://dx.doi.org/10.1016/S0014-5793\(99\)01432-5](http://dx.doi.org/10.1016/S0014-5793(99)01432-5).
- Zamocky M, Ludwig R, Peterbauer C, Hallberg BM, Divne C, Nicholls P, Haltrich D. 2006. Cellobiose dehydrogenase—a flavocytochrome from wood-degrading, phytopathogenic and saprotrophic fungi. *Curr Protein Pept Sci* 7:255–280. <http://dx.doi.org/10.2174/13892030677452367>.
- Tanaka H, Yoshida G, Baba Y, Matsumura K, Wasada H, Murata J, Agawa M, Itakura S, Enoki A. 2007. Characterization of a hydroxyl-radical-producing glycoprotein and its presumptive genes from the white-rot basidiomycete *Phanerochaete chrysosporium*. *J Biotechnol* 128:500–511. <http://dx.doi.org/10.1016/j.jbiotec.2006.12.010>.
- Henriksson G, Ander P, Pettersson B, Pettersson G. 1995. Cellobiose dehydrogenase (cellobiose oxidase) from *Phanerochaete chrysosporium* as a wood degrading enzyme—studies on cellulose, xylan and synthetic lignin. *Appl Microbiol Biotechnol* 42:790–796. <http://dx.doi.org/10.1007/BF00171963>.
- Hammel KE, Moen MA. 1991. Depolymerization of a synthetic lignin by lignin peroxidase. *Enzyme Microb Technol* 13:15–18. [http://dx.doi.org/10.1016/0141-0229\(91\)90182-A](http://dx.doi.org/10.1016/0141-0229(91)90182-A).
- Hofrichter M, Vares K, Scheibner K, Galkin S, Sipila J, Hatakka A. 1999. Mineralization and solubilization of synthetic lignin by manganese peroxidases from *Nematoloma frowardii* and *Phlebia radiata*. *J Biotechnol* 67:217–228. [http://dx.doi.org/10.1016/S0168-1656\(98\)00180-1](http://dx.doi.org/10.1016/S0168-1656(98)00180-1).
- Hammel KE, Jensen KA, Mozuch MD, Landucci LL, Tien M, Pease EA. 1993. Ligninolysis by a purified lignin peroxidase. *J Biol Chem* 268:12274–12281.
- Reiser J, Muheim A, Hardegger M, Frank G, Fiechter A. 1994. Aryl alcohol dehydrogenase from the white-rot fungus *Phanerochaete chrysosporium*: gene cloning, sequence analysis, expression and purification of recombinant protein. *J Biol Chem* 269:28152–28159.
- Ichinose H. 2013. Cytochrome P450 of wood-rotting basidiomycetes and biotechnological applications. *Biotechnol Appl Biochem* 60:71–81. <http://dx.doi.org/10.1002/bab.1061>.
- Janse BJH, Gaskell J, Akhtar M, Cullen D. 1998. Expression of *Phanerochaete chrysosporium* genes encoding lignin peroxidases, manganese peroxidases, and glyoxal oxidase in wood. *Appl Environ Microbiol* 64:3536–3538.
- Martinez D, Larrondo LF, Putnam N, Sollewijn Gelpke MD, Huang K, Chapman J, Helfenbein KG, Ramaiya P, Detter JC, Larimer F, Coutinho PM, Henrissat B, Berka R, Cullen D, Rokhsar D. 2004. Genome sequence of the lignocellulose degrading fungus *Phanerochaete chrysosporium* strain RP78. *Nat Biotechnol* 22:695–700. <http://dx.doi.org/10.1038/nbt967>.
- Gaskell J, Marty A, Mozuch M, Kersten PJ, Splinter BonDurant S, Sabat G, Azarpira A, Ralph J, Skyba O, Mansfield SD, Blanchette RA, Cullen D. 2014. Influence of *Populus* genotype on gene expression by the wood decay fungus *Phanerochaete chrysosporium*. *Appl Environ Microbiol* 80:5828–5835. <http://dx.doi.org/10.1128/AEM.01604-14>.
- Vanden Wymelenberg A, Gaskell J, Mozuch M, BonDurant SS, Sabat G, Ralph J, Skyba O, Mansfield SD, Blanchette RA, Grigoriev IV, Kersten PJ, Cullen D. 2011. Significant alteration of gene expression in wood decay fungi *Postia placenta* and *Phanerochaete chrysosporium* by plant species. *Appl Environ Microbiol* 77:4499–4507. <http://dx.doi.org/10.1128/AEM.00508-11>.
- Vanden Wymelenberg A, Gaskell J, Mozuch M, Sabat G, Ralph J, Skyba O, Mansfield SD, Blanchette RA, Martinez D, Grigoriev I, Kersten PJ, Cullen D. 2010. Comparative transcriptome and secretome analysis of wood decay

- fungi *Postia placenta* and *Phanerochaete chrysosporium*. Appl Environ Microbiol 76:3599–3610. <http://dx.doi.org/10.1128/AEM.00058-10>.
22. Vanden Wymelenberg A, Minges P, Sabat G, Martinez D, Aerts A, Salamov A, Grigoriev I, Shapiro H, Putnam N, Belinky P, Dosoretz C, Gaskell J, Kersten P, Cullen D. 2006. Computational analysis of the *Phanerochaete chrysosporium* v2.0 genome database and mass spectrometry identification of peptides in ligninolytic cultures reveals complex mixtures of secreted proteins. Fungal Genet Biol 43:343–356. <http://dx.doi.org/10.1016/j.fgb.2006.01.003>.
  23. Vanden Wymelenberg A, Gaskell J, Mozuch M, Kersten P, Sabat G, Martinez D, Cullen D. 2009. Transcriptome and secretome analyses of *Phanerochaete chrysosporium* reveal complex patterns of gene expression. Appl Environ Microbiol 75:4058–4068. <http://dx.doi.org/10.1128/AEM.00314-09>.
  24. Ralph J, Akiyama T, Kim H, Lu FC, Schatz PF, Marita JM, Ralph SA, Reddy MSS, Chen F, Dixon RA. 2006. Effects of coumarate 3-hydroxylase down-regulation on lignin structure. J Biol Chem 281:8843–8853. <http://dx.doi.org/10.1074/jbc.M511598200>.
  25. Hunt CG, Houtman CJ, Jones DC, Kitin P, Korripally P, Hammel KE. 2013. Spatial mapping of extracellular oxidant production by a white rot basidiomycete on wood reveals details of ligninolytic mechanism. Environ Microbiol 15:956–966. <http://dx.doi.org/10.1111/1462-2920.12039>.
  26. Tien M, Kirk TK. 1988. Lignin peroxidase of *Phanerochaete chrysosporium*. Methods Enzymol 161:238–249. [http://dx.doi.org/10.1016/0076-6879\(88\)61025-1](http://dx.doi.org/10.1016/0076-6879(88)61025-1).
  27. Srebotnik E, Messner K. 1994. A simple method that uses differential staining and light microscopy to assess the selectivity of wood delignification by white rot fungi. Appl Environ Microbiol 60:1383–1386.
  28. Ohm RA, Riley R, Salamov A, Min B, Choi IG, Grigoriev IV. 2014. Genomics of wood-degrading fungi. Fungal Genet Biol 72:82–90. <http://dx.doi.org/10.1016/j.fgb.2014.05.001>.
  29. Drummen GPC, Gadella BM, Post JA, Brouwers JF. 2004. Mass spectrometric characterization of the oxidation of the fluorescent lipid peroxidation reporter molecule C11-BODIPY581/591. Free Radic Biol Med 36:1635–1644. <http://dx.doi.org/10.1016/j.freeradbiomed.2004.03.014>.
  30. Stewart P, Cullen D. 1999. Organization and differential regulation of a cluster of lignin peroxidase genes of *Phanerochaete chrysosporium*. J Bacteriol 181:3427–3432.
  31. Kersten P, Cullen D. 2007. Extracellular oxidative systems of the lignin-degrading basidiomycete *Phanerochaete chrysosporium*. Fungal Genet Biol 44:77–87. <http://dx.doi.org/10.1016/j.fgb.2006.07.007>.
  32. Jensen KA, Evans KM, Kirk TK, Hammel KE. 1994. Biosynthetic pathway for veratryl alcohol in the ligninolytic fungus *Phanerochaete chrysosporium*. Appl Environ Microbiol 60:709–714.
  33. Lapadatescu C, Ginies C, Le Quere JL, Bonnarne P. 2000. Novel scheme for biosynthesis of aryl metabolites from L-phenylalanine in the fungus *Bjerkandera adusta*. Appl Environ Microbiol 66:1517–1522. <http://dx.doi.org/10.1128/AEM.66.4.1517-1522.2000>.
  34. Jeffers MR, McRoberts WC, Harper DB. 1997. Identification of a phenolic 3-O-methyltransferase in the lignin-degrading fungus *Phanerochaete chrysosporium*. Microbiology 143:1975–1981. <http://dx.doi.org/10.1099/00221287-143-6-1975>.
  35. Kapich AN, Romanovet ES, Voit SP. 1990. The content and fatty acid composition of lipids in the mycelium of wood-destroying basidiomycetes. Mikol Fitopatol 24:51–56. (In Russian.)
  36. Kapich AN, Korneichik TV, Hatakka A, Hammel KE. 2010. Oxidizability of unsaturated fatty acids and of a non-phenolic lignin structure in the manganese peroxidase-dependent lipid peroxidation system. Enzyme Microb Technol 46:136–140. <http://dx.doi.org/10.1016/j.enzmictec.2009.09.014>.
  37. Watanabe T, Katayama S, Enoki M, Honda YH, Kuwahara M. 2000. Formation of acyl radical in lipid peroxidation of linoleic acid by manganese-dependent peroxidase from *Ceriporiopsis subvermisporea* and *Bjerkandera adusta*. Eur J Biochem 267:4222–4231. <http://dx.doi.org/10.1046/j.1432-1033.2000.01469.x>.
  38. Fernandez-Fueyo E, Ruiz-Duenas FJ, Ferreira P, Floudas D, Hibbett DS, Canessa P, Larrondo LF, James TY, Seelenfreund D, Lobos S, Polanco R, Tello M, Honda Y, Watanabe T, Watanabe T, Ryu JS, Kubicek CP, Schmoll M, Gaskell J, Hammel KE, St John FJ, Vanden Wymelenberg A, Sabat G, Splinter BonDurant S, Syed K, Yadav JS, Doddapaneni H, Subramanian V, Lavin JL, Oguiza JA, Perez G, Pisabarro AG, Ramirez L, Santoyo F, Master E, Coutinho PM, Henrissat B, Lombard V, Magnuson JK, Kues U, Hori C, Igarashi K, Samejima M, Held BW, Barry KW, LaButti KM, Lapidus A, Lindquist EA, Lucas SM, Riley R, et al. 2012. Comparative genomics of *Ceriporiopsis subvermisporea* and *Phanerochaete chrysosporium* provide insight into selective ligninolysis. Proc Natl Acad Sci U S A 109:5458–5463. <http://dx.doi.org/10.1073/pnas.1119912109>.
  39. Watanabe T, Tsuda S, Nishimura H, Honda Y, Watanabe T. 2010. Characterization of a  $\Delta 12$ -fatty acid desaturase gene from *Ceriporiopsis subvermisporea*, a selective lignin-degrading fungus. Appl Microbiol Biotechnol 87:215–224. <http://dx.doi.org/10.1007/s00253-010-2438-1>.
  40. Hammel KE, Kapich AN, Jensen KA, Ryan ZC. 2002. Reactive oxygen species as agents of wood decay by fungi. Enzyme Microb Technol 30:445–453. [http://dx.doi.org/10.1016/S0141-0229\(02\)00011-X](http://dx.doi.org/10.1016/S0141-0229(02)00011-X).
  41. Larrondo LF, Salas L, Melo F, Vicuna R, Cullen D. 2003. A novel extracellular multicopper oxidase from *Phanerochaete chrysosporium* with ferroxidase activity. Appl Environ Microbiol 69:6257–6263. <http://dx.doi.org/10.1128/AEM.69.10.6257-6263.2003>.
  42. Gómez-Toribio V, García-Martin AB, Martínez MJ, Martínez AT, Guillén F. 2009. Induction of extracellular hydroxyl radical production by white-rot fungi through quinone redox cycling. Appl Environ Microbiol 75:3944–3953. <http://dx.doi.org/10.1128/AEM.02137-08>.
  43. Korripally P, Timokhin VI, Houtman CJ, Mozuch MD, Hammel KE. 2013. Evidence from *Serpula lacrymans* that 2,5-dimethoxyhydroquinone is a lignocellulolytic agent of divergent brown rot basidiomycetes. Appl Environ Microbiol 79:2377–2383. <http://dx.doi.org/10.1128/AEM.03880-12>.
  44. Bolton JL, Trush MA, Penning TM, Dryhurst G, Monks TJ. 2000. Role of quinones in toxicology. Chem Res Toxicol 13:135–160. <http://dx.doi.org/10.1021/tx9902082>.
  45. Thuillier A, Chibani K, Belli G, Herrero E, Dumarçay S, Gerardin P, Kohler A, Deroy A, Dhalleine T, Bchini R, Jacquot JP, Gelhaye E, Morel-Rouhier M. 2014. Transcriptomic responses of *Phanerochaete chrysosporium* to oak acetic extracts: focus on a new glutathione transferase. Appl Environ Microbiol 80:6316–6327. <http://dx.doi.org/10.1128/AEM.02103-14>.
  46. Park J, Lee S, Choi J, Ahn K, Park B, Park J, Kang S, Lee YH. 2008. Fungal cytochrome P450 database. BMC Genomics 9:402. <http://dx.doi.org/10.1186/1471-2164-9-402>.
  47. Yadav JS, Doddapaneni H, Subramanian V. 2006. P450ome of the white rot fungus *Phanerochaete chrysosporium*: structure, evolution and regulation of expression of genomic P450 clusters. Biochem Soc Trans 34:1165–1169. <http://dx.doi.org/10.1042/BST0341165>.
  48. van den Brink J, de Vries RP. 2011. Fungal enzyme sets for plant polysaccharide degradation. Appl Microbiol Biotechnol 91:1477–1492. <http://dx.doi.org/10.1007/s00253-011-3473-2>.
  49. Lombard V, Golaconda Ramulu H, Drula E, Coutinho PM, Henrissat B. 2014. The carbohydrate-active enzymes database (CAZy) in 2013. Nucleic Acids Res 42:D490–D495. <http://dx.doi.org/10.1093/nar/gkt1178>.
  50. Lévasscur A, Drula E, Lombard V, Coutinho PM, Henrissat B. 2013. Expansion of the enzymatic repertoire of the CAZy database to integrate auxiliary redox enzymes. Biotechnol Biofuels 6:41. <http://dx.doi.org/10.1186/1754-6834-6-41>.
  51. Westereng B, Ishida T, Vaaje-Kolstad G, Wu M, Eijsink VG, Igarashi K, Samejima M, Stahlberg J, Horn SJ, Sandgren M. 2011. The putative endoglucanase PcGH61D from *Phanerochaete chrysosporium* is a metal-dependent oxidative enzyme that cleaves cellulose. PLoS One 6:e27807. <http://dx.doi.org/10.1371/journal.pone.0027807>.
  52. Yakovlev I, Vaaje-Kolstad G, Hietala AM, Stefanczyk E, Solheim H, Fossdal CG. 2012. Substrate-specific transcription of the enigmatic GH61 family of the pathogenic white-rot fungus *Heterobasidion irregulare* during growth on lignocellulose. Appl Microbiol Biotechnol 95:979–990. <http://dx.doi.org/10.1007/s00253-012-4206-x>.
  53. Bey M, Zhou S, Poidevin L, Henrissat B, Coutinho PM, Berrin JG, Sigoillot JC. 2013. Cello-oligosaccharide oxidation reveals differences between two lytic polysaccharide monooxygenases (family GH61) from *Podospira anserina*. Appl Environ Microbiol 79:488–496. <http://dx.doi.org/10.1128/AEM.02942-12>.
  54. Quinlan RJ, Sweeney MD, Lo Leggio L, Otten H, Poulsen JC, Johansen KS, Krogh KB, Jorgensen CI, Tovborg M, Anthonisen A, Tryfona T, Walter CP, Dupree P, Xu F, Davies GJ, Walton PH. 2011. Insights into the oxidative degradation of cellulose by a copper metalloenzyme that exploits biomass components. Proc Natl Acad Sci U S A 108:15079–15084. <http://dx.doi.org/10.1073/pnas.1105776108>.
  55. Agger JW, Isaksen T, Varnai A, Vidal-Melgosa S, Willats WG, Ludwig R, Horn SJ, Eijsink VG, Westereng B. 2014. Discovery of LPMO activity

- on hemicelluloses shows the importance of oxidative processes in plant cell wall degradation. *Proc Natl Acad Sci U S A* 111:6287–6292. <http://dx.doi.org/10.1073/pnas.1323629111>.
56. Kohler A, Kuo A, Nagy LG, Morin E, Barry KW, Buscot F, Canback B, Choi C, Cichocki N, Clum A, Colpaert J, Copeland A, Costa MD, Dore J, Floudas D, Gay G, Giralda M, Henrissat B, Herrmann S, Hess J, Hogberg N, Johansson T, Khouja HR, LaButti K, Lahrmann U, Levasseur A, Lindquist EA, Lipzen A, Marmeisse R, Martino E, Murat C, Ngan CY, Nehls U, Plett JM, Pringle A, Ohm RA, Perotto S, Peter M, Riley R, Rineau F, Ruytinx J, Salamov A, Shah F, Sun H, Tarkka M, Tritt A, Veneault-Fourrey C, Zuccaro A, Mycorrhizal Genomics Initiative C, Tunlid A, et al. 2015. Convergent losses of decay mechanisms and rapid turnover of symbiosis genes in mycorrhizal mutualists. *Nat Genet* 47:410–415. <http://dx.doi.org/10.1038/ng.3223>.